1   **Genetic evidence for erythrocyte receptor glycophorin B expression levels defining a**

2   **dominant *Plasmodium falciparum* invasion pathway into human erythrocytes**

3

4   Selasi Dankwa[a]*, Mudit Chaand[a], Usheer Kanjee[a], Rays H.Y. Jiang[a†], Luis V. Nobre[b],

5   Jonathan M. Goldberg[a], Amy K. Bei[a], Mischka A. Moechtar[a], Christof Grüring[a],

6   Ambroise D. Ahouidi[c], Daouda Ndiaye[c], Tandakha N. Dieye[c], Souleymane Mboup[c],

7   Michael P. Weekes[b] Manoj T. Duraisingh[a, #]

8

9   [a]Department of Immunology and Infectious Diseases, Harvard T.H. Chan School of

10   Public Health, Boston, MA

11   [b]Cambridge Institute for Medical Research, University of Cambridge, Cambridge, UK

12   [c]Laboratory of Bacteriology and Virology, Le Dantec Hospital, Cheikh Anta Diop

13   University, Dakar, Senegal

14

15   Running title: Glycophorin B-mediated *P. falciparum* invasion

16

17   [#]To whom correspondence should be addressed: Manoj T. Duraisingh

18   mduraisi@hsph.harvard.edu

19

20   Present addresses:

21   *Center for Infectious Disease Research, Seattle, WA

22   [†]Department of Global Health and Center for Drug Discovery and Innovation, University

23   of South Florida, Tampa, FL

24   **Abstract**

25   *Plasmodium falciparum*, the parasite that causes the deadliest form of malaria, has

26   evolved multiple proteins known as invasion ligands that bind to specific erythrocyte

27   receptors to facilitate invasion of human erythrocytes. The EBA-175/glycophorin A

28   (GPA) and Rh5/basigin ligand-receptor interactions, referred to as invasion pathways,

29   have been the subject of intense study. In this study, we focused on the lesser

30   characterized sialic acid-containing receptors glycophorin B (GPB) and glycophorin C

31   (GPC). Through bioinformatic analysis, we identified extensive variation in glycophorin

32   B transcript (GYPB) levels in individuals from Benin, suggesting selection from malaria

33   pressure. To elucidate the importance of the GPB and GPC receptors relative to the well-

34   described EBA-175/GPA invasion pathway, we used an *ex vivo* erythrocyte culture

35   system to decrease expression of GPA, GPB or GPC via lentiviral short hairpin RNA

36   transduction of erythroid progenitor cells, with global surface proteomic profiling. We

37   assessed parasite invasion efficiency into knock down cells using a panel of wild type *P.*

38   *falciparum* laboratory strains and invasion ligand knockout lines, as well as *P. falciparum*

39   Senegalese clinical isolates and a short-term culture-adapted strain. For this, we

40   optimized an invasion assay suitable for use with small numbers of erythrocytes. We

41   found that all laboratory strains and the majority of field strains tested were dependent on

42   GPB expression level for invasion. Collective data suggest that the GPA and GPB

43   receptors are of greater importance than the GPC receptor, supporting a hierarchy of

44   erythrocyte receptor usage in *P. falciparum*.

45

46

Introduction

Malaria is a disease of major global health importance that is caused by parasites of the genus *Plasmodium*, of which *Plasmodium falciparum* is the most virulent (1). The asexual erythrocytic stage of the parasite life cycle is responsible for the symptoms associated with malaria (1). A key step during this stage is parasite invasion of erythrocytes mediated by interactions between parasite invasion ligands and their cognate erythrocyte receptors, which define invasion pathways. Across *Plasmodium* species, invasion ligands are grouped into two families – the Duffy binding-like or Erythrocyte binding-like (DBL/EBL) family, and the Reticulocyte binding-like (RBL) family (2–4). *P. falciparum* has four EBL ligands – EBA-175, EBL-1 (PEBL), EBA-140 (BAEBL) and EBA-181 (JESEBL) and five RBL ligands – Rh1, Rh2a, Rh2b, Rh4 and Rh5. Of these, the cognate receptors of five invasion ligands are known – glycophorin A, B and C, which bind EBA-175 (5), EBL-1 (6, 7) and EBA-140 (8, 9) respectively, and complement receptor 1 (CR1) and basigin (BSG), receptors for Rh4 (10, 11) and Rh5 (12) respectively.

Invasion pathways can be classified according to their dependence on the presence of sialic acid on receptors; pathways involving the EBL invasion ligands and Rh1 are reliant on sialic acid (sialic acid-dependent invasion pathways), while those involving the remaining RBL ligands are not (sialic acid-independent invasion pathways). Although *P. falciparum* has an extensive array of invasion pathways, not all are utilized at the same time. The set of dominant invasion pathways used during invasion is strain-dependent and has led to a broad classification of *P. falciparum* strains as sialic acid-dependent or -independent. However, laboratory-adapted strains have the

3

70 ability to switch invasion pathway usage when specific receptors or determinants of

71 interaction are absent from the erythrocyte surface (13, 14). Furthermore, field isolates

72 commonly utilize different sets of invasion pathways (15–20). The virulence of *P.*

73 *falciparum* has been partly attributed to its extensive set of invasion pathways, which

74 enable it to efficiently invade diverse host erythrocytes harboring different receptor

75 polymorphisms.

76 Most recently, the Rh5/BSG sialic acid-independent invasion pathway has

77 received the greatest attention owing to the essentiality of the Rh5/BSG invasion pathway

78 (12, 20). Other studies have also shown that the EBA-175/GPA sialic acid-dependent

79 invasion pathway plays a significant role in both sialic acid-dependent and sialic acid-

80 independent strains (21–23). Importantly, naturally occurring anti-EBA-175 and anti-Rh5

81 invasion-inhibitory antibodies have been identified in malaria-exposed individuals (24–

82 27).

83 Lesser characterized are the EBA-140/GPC sialic acid-dependent invasion

84 pathway (8, 9, 28, 29), and the sialic acid-dependent parasite invasion ligand EBA-181

85 for which no receptor has been identified (30–32). The EBL-1/GPB invasion pathway has

86 also been poorly characterized and there are contradictory reports regarding the

87 importance of GPB. One study reported a complete block in invasion of the sialic acid-

88 independent strain, 7G8, into GPB null (S-s-U-) erythrocytes (33), although a prior study

89 showed little inhibition of this strain (34). A subsequent study showed a 40-87% range in

90 invasion efficiency into S-s-U- erythrocytes from five donors (35). Donor to donor blood

91 group differences and differences in receptors may contribute to the variable invasion

92   phenotypes of GPB null cells and underscore a potential weakness of comparing non-

93   isogenic mutant and wild type erythrocytes.

94   In a search for novel signatures of *P. falciparum* infection, we performed

95   computational analysis of a published dataset of transcriptomic profiles from malaria-

96   infected and healthy Beninese children (36), which led to the discovery that there is wide

97   variation in GYPB transcripts in healthy individuals. This finding provided the impetus

98   for a detailed study of the use of the GPB receptor in *P. falciparum* invasion. In this

99   study, we used an erythrocyte reverse genetics system (37) to specifically knock down

100 levels of expression of the sialic acid-dependent receptors GPA, GPB and GPC. We

101 report that GPB is a key determinant of *P. falciparum* invasion.

102

103 **Materials and Methods**

104 **Bioinformatic analyses.** A set of 314 host genes with known or potential roles in

105 parasite invasion was defined by combining erythroblast-specific genes from HaemAtlas

106 (38) with blood group genes from the International Society of Blood Transfusion

107 (http://www.isbtweb.org/). Whole-blood raw transcriptomic data from 61 healthy

108 Beninese children (36) were obtained from the Gene Expression Omnibus (GSE34404).

109 Two hundred and thirty-eight genes from the erythroblast-specific/blood group set

110 defined above are expressed in the Benin dataset. This subset was background-corrected

111 using the detection *p*-value and quantile normalized using *limma* (39). The 95th to 5th

112 quantile ratios were calculated to identify the most variable transcripts.

113 *Ex vivo* **culture of erythrocytes.** $3\text{-}10\text{x}10^5$ bone marrow-derived $CD34^+$ hematopoietic

114 stem cells (HSCs; Lonza) or $CD34^+$ cells derived from peripheral blood of GCSF-

115   stimulated donors (obtained from the HSCI-Boston Children's Hospital FACS Core)

116   were cultured in Iscove's modified Dulbecco's medium (IMDM, Biochrom)

117   supplemented with glutamine (Sigma-Aldrich), holo-human transferrin (Scipac),

118   recombinant human insulin (Sigma-Aldrich), heparin Choay (USBioAnalyzed) and 5%

119   solvent/detergent virus-inactivated plasma (Octaplas, Octapharma) as described (40) with

120   the following modifications. On day 6 or 7, cells were transduced with lentivirus

121   harboring short hairpin RNA (shRNA) against GYPA (Clone ID: TRCN0000116453),

122   GYPB (Clone ID: TRCN0000084081) or GYPC (Clone ID: TRCN0000083398) or the

123   empty vector (pLKO). Lentiviral particles were either prepared as previously described

124   (37) or obtained from the RNAi Platform (Broad Institute). Transduction and subsequent

125   selection on 2 µg/ml puromycin dihydrochloride (Sigma-Aldrich) were performed as

126   formerly described (41). From day 12 or 13 to day 18, cells were co-cultured on a

127   murine MS-5 stromal cell layer at a cell density of $3\text{-}6\text{x}10^5$ cells/ml as described (42, 43).

128   On day 18, cells were re-plated on a fresh MS-5 stromal cell layer. Cells were harvested

129   on either day 17 or 18 or day 20 and passed through a 5 µm Supor filter (Pall) to remove

130   residual nucleated cells. Filtered, enucleated cells were stored at 4°C in incomplete RPMI

131   [RPMI-1640 (Sigma-Aldrich) supplemented with 25 mM HEPES and 50 mg L^{-1}

132   hypoxanthine] until use in subsequent experiments.

133   **Flow cytometry-based measurement of erythrocyte receptor expression.**

134   Erythrocytes were washed three times in PBS-3% BSA blocking buffer, then pelleted in a

135   96-well plate at $5\text{x}10^5$ erythrocytes per well (cultured erythrocytes) or $1\text{x}10^6$ (peripheral

136   erythrocytes) and finally resuspended in 50 µl (cultured erythrocytes) or 100 µl

137   (peripheral erythrocytes) of PBS-3% BSA or the appropriate antibody solution. The

138 following antibodies were used at the indicated dilutions: phycoerythrin(PE)-conjugated

139 anti-DARC (1:10, Miltenyi Biotec), anti-CD71-PE (1:10, Miltenyi Biotec), fluorescein

140 isothiocyanate(FITC)-conjugated anti-GPA (1:50, Clone 2B7, STEMCELL

141 Technologies), anti-GPC-FITC (1:500, BRIC 10, Santa Cruz), anti-band 3-FITC [1:100,

142 BRIC 6-FITC, International Blood Group Reference Laboratory (IBGRL)], anti-BSG

143 [1:1,000, Clone MEM-M6/6, Axxora (Exbio)], anti-CR1 (1:200, Santa Cruz), anti-DAF

144 (1:3,000, BRIC 216, IBGRL), anti-RhD (1:20, BRAD3-FITC, IBGRL), and anti-GPA/B

145 (1:8,000, Clone E3, Sigma-Aldrich). To measure GPB expression, erythrocytes were

146 treated with 1 mg/ml trypsin (Sigma-Aldrich) to remove GPA before incubation in the

147 GPA/B antibody. For measurement of GPA and GPC expression in Senegal, the

148 following probes were used in addition to the aforementioned antibodies: anti-GPA –

149 BRIC 256 IgG (IBGRL, 1:100,000) and BRIC 256-FITC fab fragment (1:20); anti-GPC –

150 BRIC 10 IgG (IBGRL, 1:500,000), BRIC 10-FITC fab fragment (1:100) and BRIC 4 IgG

151 (IBGRL, 1:8,000). Fab fragments were produced from whole IgG by papain digestion

152 (Pierce Fab Preparation kit; Thermo Scientific) and FITC-labelled (ProtOn Fluorescein

153 Labelling kit, Vector Laboratories), followed by extensive dialysis in PBS.

154   Cells were incubated for 1 h at room temperature and washed three times in

155 blocking buffer. Unstained cells and cells stained with directly conjugated antibodies

156 were resuspended in 100 µl PBS for analysis on the MACSQuant flow cytometer [in

157 Boston (Miltenyi Biotec)] or the BD FACScalibur [in Senegal (BD Biosciences)].

158 Erythrocytes incubated with all other antibodies were then incubated in anti-mouse IgG-

159 Alexa Fluor 488 (1:1,000, Life Technologies) for 30 min at room temperature. Control

160 samples with no prior antibody incubation were incubated in either anti-mouse IgG2a-PE

161   (1:10, Miltenyi Biotec) or anti-mouse IgG-Alexa Fluor 488. Cells were washed twice

162   and subjected to flow cytometric analyses. The data were analyzed using FlowJo 4 v.

163   10.0.7 for flow cytometry done in Boston or FlowJo v. 8.8.6 for flow cytometry done in

164   Senegal.

165   **Quantitative cell surface proteomics.** pLKO control, GPA knockdown, GPB

166   knockdown and GPC knockdown cultured erythrocytes (cRBCs) were prepared as

167   described earlier in the text. The following sets of cells were labeled by aminooxy-biotin

168   as described previously (44, 45) – pLKO cRBCs: 10.2 x 10^6 cells (in duplicate); GPA

169   KD: 16.2 x 10^6 cells; GPB KD: 3.5 x 10^6 cells; GPC KD: 11.2 x 10^6 cells; peripheral

170   RBCs: 10.0 x 10^6 cells (in duplicate).

171   Briefly, surface sialic acid residues were oxidized with sodium meta-periodate

172   (Thermo) then biotinylated with aminooxy-biotin (Biotium). The reaction was quenched,

173   and the biotinylated cells incubated in a 1% Triton X-100 lysis buffer. Biotinylated

174   glycoproteins were enriched with high affinity streptavidin agarose beads (Pierce) and

175   washed extensively. Captured protein was denatured with dithiotreitol (Sigma-Aldrich),

176   alkylated with iodoacetamide (IAA, Sigma) and digested on-bead with trypsin (Promega)

177   in 200 mM HEPES pH 8.5 for 3 hours. Tryptic peptides were collected and labeled using

178   TMT reagents (Thermo Scientific). The reaction was quenched with hydroxylamine, and

179   TMT-labeled samples combined in a 1:1:1:1:1:1:1 ratio. Labeled peptides were enriched

180   and desalted and then 6% of the total sample was subjected to mass spectrometry.

181   Mass spectrometry data was acquired using an Orbitrap Fusion coupled with an

182   UltiMate 3000 Nano LC (Thermo). Peptides were separated on a 75 cm PepMap C18

183   column (Thermo). Peptides were separated using a 180 min gradient of 3 to 33%

8

184   acetonitrile in 0.1% formic acid at a flow rate of 200 nL/min. Each analysis used a

185   MultiNotch MS3-based TMT method (45, 46). The scan sequence began with an MS1

186   spectrum (Orbitrap analysis, resolution 120,000, 400-1400 Th, AGC target 2 x 105,

187   maximum injection time 50 ms). MS2 analysis consisted of CID (quadrupole ion trap

188   analysis, AGC 15,000, NCE 35, maximum injection time 120 ms). The top ten precursors

189   were selected for MS3 analysis, in which precursors were fragmented by HCD prior to

190   Orbitrap analysis (NCE 55, max AGC 2 x 105, maximum injection time 150 ms, isolation

191   specificity 0.5 Th, resolution 60,000).

192   **Sample collection for *ex vivo* invasion assays and erythrocyte receptor expression.**

193   Collection of clinical isolates and their experimental use were approved by the Ethics

194   Committee of the Ministry of Health in Senegal and by the Institutional Review Board of

195   the Harvard T.H. Chan School of Public Health. Sample collection was done in

196   November 2013, towards the end of the transmission season in Senegal. After informed

197   consent from patients presenting with uncomplicated malaria in Thies, Senegal, ~4 ml of

198   whole blood was collected from each patient in Sodium Citrate Vacutainers and

199   transported to Dakar, Senegal. Samples arrived in the laboratory within 6 hours of draw

200   and after washes in incomplete RPMI and removal of the buffy coat, a fraction of

201   parasitized cells was enzyme-treated with *Vibrio cholerae* neuraminidase (Sigma-

202   Aldrich), chymotrypsin (Worthington) and trypsin and placed in culture conditions until

203   invasion assay set up.

204   For measurement of erythrocyte receptor expression in healthy Senegalese, 2-3 ml of

205   whole blood was collected from healthy donors from the Senegalese National Blood

206   Transfusion Center in Dakar, Senegal. Flow cytometry was performed on the day of

207   blood collection.

208   **Parasite cultures.** *P. falciparum* cultures were maintained in human O^+ erythrocytes.

209   Parasites were grown at 2% hematocrit in complete RPMI medium (incomplete RPMI

210   supplemented with 2.57 mM sodium bicarbonate (Sigma-Aldrich), 0.25% AlbuMAX II

211   (Life Technologies) and 0.25% AB^+ serum (for *ex vivo* cultures) or 0.5% AlbuMAX II

212   for laboratory strains and the short-term culture-adapted strain. Cultures were kept at

213   37°C in a modulator incubator chamber, gassed with 1% O_2, 5% CO_2 and 94% N_2.

214   **Enzyme treatments.** Ring stage parasite cultures were washed three times in incomplete

215   RPMI and treated with 1 mg/ml trypsin, 1 mg/ml chymotrypsin and 66.7 mU/ml of

216   *Vibrio cholerae* neuraminidase for 1 h at 37°C, with gentle mixing. Enzyme-treated cells

217   were then washed twice in incomplete RPMI and once in complete RPMI, then

218   resuspended at 2% hematocrit (HCT) in complete RPMI and placed in culture.

219   **Invasion Assays.** Invasion assays were performed in half-area 96-well plates in

220   duplicate or triplicate. At the late trophozoite or schizont stage, the parasite culture was

221   resuspended and adjusted to 0.5% HCT based on hemocytometer cell counts, for *ex vivo*

222   invasion assays in Senegal, or based on volume, for invasion assays conducted in Boston.

223   GPA-, GPB- and GPC-knockdown cultured erythrocytes (cultured red blood cells;

224   cRBCs) and pLKO cRBCs were adjusted to 0.5% HCT based on hemocytometer cell

225   counts. Parasitized cells were added to cRBCs at an 80:20 ratio (see Fig. 4B). For *ex*

226   *vivo* invasion assays in Senegal, 10 μl of the total sample volume of 40 μl was used for

227   smears to determine the starting parasitemia by light microscopy. Boston-based invasion

228   assays were performed with a total sample volume of 30 μl. Assays were harvested 30-

229   40 hours post-set up by making smears or cytospin preparations, which were stained with

230   May-Grünwald and Giemsa to determine final parasitemia by light microscopy. 500-

231   2000 erythrocytes were counted, depending on the experiment. The invasion efficiency

232   based on final parasitemia was determined for each strain after normalization to pLKO

233   control cells.

234   **Statistical Analyses.** Univariate analyses were performed using GraphPad Prism v. 5.0

235   for Mac OS X. Significant differences between each knockdown group and control group

236   were determined using a one-way ANOVA and Dunnett's multiple comparison test.

237   **Data analysis for quantitative surface proteomics.** Mass spectra were processed using

238   a Sequest-based in-house software pipeline as previously described (47). Data were

239   searched using the human Uniprot database (April 2014) concatenated with common

240   contaminants, and filtered to a final protein-level false discovery rate of 1%. Proteins

241   were quantified by summing TMT reporter ion counts across all peptide-spectral matches

242   using in-house software as previously described (47), excluding peptide-spectral matches

243   with poor quality MS3 spectra (a combined signal:noise ratio of less than 250 across all

244   TMT reporter ions). For protein quantitation, reverse and contaminant proteins were

245   removed.

246   A subset of 78 membrane proteins were identified based on the presence of the

247   following criteria extracted from the UniProt (48) database (type I/II/III/IV

248   transmembrane domain, multipass transmembrane domain, GPI-anchored, lipid

249   anchored) or predictions of transmembrane helices based on the TMHMM 2.0 program

250   (49, 50). Each reporter ion channel was summed across all 78 proteins and normalized

251   assuming equal protein loading across all samples. To compare the relative abundance of

252 the membrane proteins between the pLKO cRBCs and KD cRBCs, proteins with a

253 coefficient of variation > 0.25 in the pLKO technical replicates were excluded from

254 further analysis.

255   Fold change for each protein was calculated according to signal:noise (GYP

256 KD)/average signal:noise (pLKO controls). *P*-values (Significance A) were calculated

257 and adjusted with the Benjamini-Hochberg method using Perseus v. 1.5.1.6 (51). To

258 compare the abundance of plasma membrane proteins between pLKO cRBCs and

259 peripheral RBCs, for each protein the normalized signal for each reporter channel was

260 renormalized to a total of 1 and the data were clustered using the k-means algorithm in

261 Cluster v. 3.0 with a Euclidean distance metric (52) and subsequently displayed using

262 TreeView v. 1.1.6r4 (53).

263
264
265 **Results**
266
267 **Glycophorin B transcript levels vary widely amongst healthy individuals in a**

268 **malaria-endemic region**

269   Erythrocyte receptors involved in *P. falciparum* invasion and their regulatory

270 regions harbor polymorphisms, some of which are overrepresented in malaria-endemic

271 regions and are suggested to have arisen as a consequence of the selective force of

272 malaria on the human genome. To determine if we could identify additional

273 polymorphisms that might affect *P. falciparum* infection, we performed computational

274 analysis of transcriptional profiles generated from whole blood of children in Benin,

275 published by Idaghdour *et*. *al* (36). We first defined a subset of erythroid-specific genes

276 from the transcriptome based on the HaemAtlas published by the Bloodomics

277 Consortium (38) and from known blood groups. Of 238 erythroid-specific/blood group

278 transcripts from 61 healthy children included in the analysis, we identified four genes

279 with wide expression range (95 quantile to 5 quantile ratio larger than 10, z score > 3):

280 carbonic anhydrase 1 (CA1), hemoglobin zeta chain (HBZ), RAP1 GTPase activating

281 protein (RAP1GAP) and unexpectedly, GYPB (Fig. 1A). Importantly, many transcripts

282 with little variation served as internal controls (Fig. 1A).

283   To determine if this GYPB transcript variation translated to receptor expression

284 variation, we measured the levels of GPB, as well as GPA, GPC and other blood group

285 receptors in healthy donors in the malaria endemic country of Senegal over two

286 consecutive years (Fig. 1B). The variation in surface expression of GPB in GPB-positive

287 individuals, estimated by the 95/5 quantile ratio, was ~1.5 fold above background, much

288 smaller than the transcriptional variation found in the Beninese children. We also

289 observed modest variation in surface expression of other receptors we measured, with a

290 95/5 quantile ratio ranging from ~1.2 to 3 (Fig. 1B).

291

292 **Knockdown of GPA, GPB or GPC in *ex vivo* cultured erythrocytes**

293   To understand expression level modulation of GPB in *P. falciparum* invasion and

294 to determine the importance of this receptor relative to the other major sialic acid-

295 dependent receptors, GPA and GPC, we knocked down expression of GPB in *ex vivo*

296 cRBCs via shRNA-mediated gene silencing (37). In 6-7 independent experiments, we

297 achieved approximately $53.5 \pm 8.9\%$ standard deviation (SD) knockdown (KD) of GPA

298 ($P \le 0.001$), $72.3 \pm 14.2\%$ SD KD of GPB ($P \le 0.001$) and $82.9 \pm 6.5\%$ SD KD of GPC

299 ($P \le 0.001$) (Fig. 2A and 2B), as determined by flow cytometry. We also measured the

300 expression level of all of the glycophorins (between three and seven times), and

301 following KD of each receptor, found little change in the expression levels of the others

302 by flow cytometry (Fig. 2B). We further measured surface expression by flow cytometry

303 of other known *Plasmodium* receptors (BSG, band 3, CR1 and DARC) (Fig. S1). We

304 observed a four-fold increase in band 3 levels following GPA KD as previously reported

305 (54) a two-fold increase in BSG levels on GPA KD cells, and a ~25% decrease in BSG

306 levels on GPB KD cells. Further, we found no association between GPB and BSG levels

307 by flow cytometry in Senegalese individuals (Fig. 1B). In addition, KD and pLKO

308 control cRBCs had normal erythrocyte morphology (Fig. 2C).

309

310 **Global proteomic profiling to determine the level and specificity of GPA, GPB and**

311 **GPC receptor knockdowns**

312 To establish the similarity between cRBCs and physiologically derived red blood

313 cells (pRBCs), we measured expression of 78 cell surface receptors by plasma membrane

314 profiling (PMP) on cRBCs and pRBCs (Table S1). Firstly, this analysis demonstrated the

315 reticulocyte-like nature of the cRBCs by showing that several proteins that decrease in

316 abundance during reticulocyte maturation, including CD71 (TFRC) (55, 56), CD36 (57,

317 58), ITGA4 (58), and SLC3A2 (59), were decreased in pRBCs relative to pLKO cRBCs

318 (Cluster 1; Fig. 3A). The level of expression of proteins in Cluster 2 remained

319 unchanged between pRBCs and pLKO cRBCs, while Cluster 3 proteins were enriched on

320 pRBCs, and include GPA, and GPC. (By this method we are unable to distinguish

321 between GPA and GPB peptides, thus due to the ~four-fold greater abundance of GPA

322 receptors, we assume that the signal emanates from a ratio of 4:1 for GPA:GPB.)

323   We have calculated the numbers of molecules per unit surface area of known *P.*

324   *falciparum* host receptors (46, 60–66) (Table 1), using published values of the surface

325   area of reticulocytes (142.4 ± 2.0 μm^2) and pRBCs (133.6 ± 3.0 μm^2) (46). We find that

326   the surface density of receptors between pLKO cells and pRBCs for all known receptors,

327   are within three-fold of each other, except for CR1 which is ~five-fold lower on pLKO

328   cRBCs. GPA/GPB and GPC are found at lower levels on pLKO cells, while BSG is the

329   only major receptor that is found at a higher level. The lower density of GPA/ GPB and

330   GPC on pLKO cells suggests that further limitation of receptor densities by knockdown

331   will elicit receptor densities significantly lower than those observed on pRBCs (Table 1).

332   To ensure that the specificity of invasion phenotypes would result specifically

333   from the receptors that were depleted, we made a comparison of pLKO and KD cRBCs.

334   As expected, GPA and GPC were reduced in the GPA and GPC KD cRBCs respectively

335   (Fig. 3B, 3D). As mentioned earlier, GPA and GPB peptides are indistinguishable;

336   therefore GPB depletion in the GPB KD cells was not observable by this analysis. Of all

337   the known receptors considered, only BSG levels were reduced in any of the KDs (albeit

338   at borderline significance, $P = 0.047$) (Table S1, Fig. 3C), in GPB KD cells. Calculated

339   surface densities of BSG on GPB KD cells are comparable to those found on pRBCs

340   (Table 1), suggesting that BSG is not limited to levels that would contribute to an

341   invasion phenotype. This analysis also revealed other proteins that have significantly

342   altered levels in the pLKO cRBCs relative to KD cRBCs (Fig. 3B-D, Table S2). To date,

343   no role in invasion has been described for these proteins.

344   Interestingly, band 3 (SLC4A1) levels were not significantly elevated by

345   proteomic analysis on GPA KD cells (Fig. 3B), in contrast to the significant increase in

346   band 3 levels determined by flow cytometry (Fig. S1) (67, 68). One potential explanation

347   for the discrepancy is that knockdown of GPA improves accessibility of the band 3

348   antibody to its epitope during flow cytometry measurements.

349

350   **A scaled-down assay for measuring erythrocyte invasion efficiency**

351   To enable us assess invasion profiles of as many *P. falciparum* strains as possible,

352   we developed a scaled-down invasion assay that makes use of small numbers of cells of

353   interest (Fig. 4A).   In our assay design, a *P. falciparum* culture treated with

354   neuraminidase (N), trypsin (T) and chymotrypsin (C), constituting donor cells, is added

355   to cells of interest (acceptor cells) in an 80:20 ratio and parasitemia is determined after a

356   single round of invasion. We used the 80:20 ratio of donor to acceptor cells over other

357   ratios because the 80:20 ratio allowed us to use a limited number of cultured

358   erythrocytes, yet gave us a reasonable, measurable final parasitemia of 3% when

359   assessing invasion of 3D7 into pLKO control cells with a starting parasitemia of ~2%

360   (Fig. 4B). The success of this scaled-down assay depends on effective NTC treatment to

361   prevent re-invasion into donor cells, careful counting of acceptor cells (achieved with a

362   hemocytometer) and a reasonable starting parasitemia in the donor culture (ideally 2.5%),

363   since only 20% of the cells in each sample have intact receptors for invasion.

364

365   **Glycophorin B is a major receptor used by *P. falciparum* laboratory strains**

366   To assess the relative importance of GPB in invasion, we tested invasion of KD

367   cRBCs by a panel of wild type *P. falciparum* laboratory-adapted strains and invasion

368   ligand deletion strains. Using our scaled-down invasion assay, we observed decreased

16

369   invasion of the sialic acid-dependent strain, Dd2, into GPB KD cRBCs (56.4 ± 24.2%

370   SD) as well as GPA KD cRBCs (72.9 ± 18.3%, SD) as previously reported (37), but no

371   change in invasion of GPC KD cells (91.8 ± 8.2% SD) relative to pLKO control cells

372   (Table 2).

373   It has been shown that strain 3D7 uses the sialic acid-dependent EBA-175/GPA

374   invasion pathway to some extent (23). We did not observe a decrease in invasion of 3D7

375   into GPA KD cRBCs consistent with a previous report (37), however, the parent 3D7

376   strain and the derived invasion ligand deletion lines, 3D7ΔEBA-175 and 3D7ΔRh2b, had

377   decreased invasion into GPB KD cRBCs (Table 2). This decrease reached statistical

378   significance for 3D7 (66.6 ± 23.3% SD and 3D7ΔRh2b (60.5% ± 26.6% SD), indicating

379   that in 3D7, the GPB receptor is more important than the GPA receptor. None of the 3D7

380   strains showed decreased invasion into GPC KD cRBCs (Table 2), suggesting a lesser

381   role in invasion for this receptor.

382   Like 3D7, the sialic acid-independent strains 7G8 and HB3 showed decreased

383   invasion of GPB KD cells, though this decrease was not statistically significant (Table 2).

384   We did not observe decreased invasion of 7G8 or HB3 into GPA or GPC KD cRBCs,

385   relative to pLKO cRBCs. Altogether, our data suggest that GPB is important for invasion

386   by the tested sialic acid-dependent and sialic acid-independent laboratory strains of *P.*

387   *falciparum.*

388

389   **Many *P. falciparum* field isolates use glycophorin B for invasion.**

390   To determine if GPB is important in invasion by field isolates, we assessed

391   invasion of a culture-adapted Senegalese isolate and fresh clinical isolates from Senegal

392   into KD cRBCs (Tables 2 and 3). Sen51, a short-term culture-adapted strain, which was

393   sensitive to neuraminidase treatment [defined as invasion efficiency of less than 60% into

394   neuraminidase(Nm)-treated pRBCs that are devoid of sialic acid (Table S3)], showed

395   decreased invasion into GPB KD cRBCs (58.8 ± 16.8% SD) compared to GPA KD

396   cRBCs (109.7 ± 28.3% SD) and GPC KD cRBCs (113.0 ± 3.6% SD) (Table 2).

397   For invasion of fresh clinical isolates, five out of eight strains had less than 60%

398   invasion into GPB KD cRBCs as well as GPA KD cRBCs, while none of the five had

399   less than 60% invasion into GPC KD cRBCs relative to pLKO cRBCs (Table 3). Of these

400   five isolates, three were sensitive to Nm-treated pRBCs (Th303, Th305 and Th306),

401   while two were resistant (Th304 and Th312). Two other isolates, which had decreased

402   invasion only into GPC KD cRBCs were sensitive to Nm-treated pRBCs (Th266 and

403   Th268), bringing the proportion of Nm-sensitive strains to 75% (six out of eight strains).

404   Invasion into GPB KD cells ranged from 36.7 ± 5.8% SD to 118.0 ± 66.4% SD, while the

405   range for GPA KD cells was 28.5 ± 3.5% SD to 110.4 ± 60.7% SD and for GPC KD

406   cells, 52.5 ± 16.4% SD to 93.5 ± 42.2% SD (Table 3). Overall, our results indicate that

407   for field isolates, GPB is of comparable importance in invasion as GPA, and more

408   utilized than GPC for most strains tested, though there is more heterogeneity in receptor

409   usage for field isolates than lab lines. Furthermore, there is not a simple relationship

410   between sialic acid-dependence and the invasion phenotype into KD cRBCs.

411

412   **Discussion**
413   In this study we have used erythrocyte reverse genetics in an isogenic background

414   to specifically and comparatively assess the use of three major sialylated erythrocyte

415   receptors – GPA, GPB and GPC – in invasion of erythrocytes by *P. falciparum*

18

416   laboratory-adapted and field strains. We used genetically altered cRBCs to evaluate the

417   contribution of specific invasion ligands in isogenic cells in *ex vivo* parasite invasion

418   assays. This contrasts with previous studies, which depend on enzyme-treated cells and

419   non-isogenic naturally occurring mutant erythrocytes to reveal invasion pathways (54).

420   The cRBCs used in this study express the full complement of *P. falciparum* receptors and

421   are of a relatively homogeneous age, though their reticulocyte-like nature results in some

422   differences in surface receptor abundance, relative to pRBCs. Nevertheless, we achieved

423   limiting numbers of receptors on KD cells, enabling us to determine the relative

424   importance of specific receptors. In comparing invasion into GPA, GPB, and GPC KD

425   cells, we observed a dependence on GPB by both sialic acid-dependent and sialic acid-

426   independent laboratory strains; this reliance on GPB was greater than GPA, which is used

427   by many laboratory strains regardless of sialic acid-dependence (21, 23). Our data also

428   suggest that the GPC receptor is less important for invasion in most strains tested.

429   Bioinformatic analysis of transcriptional profiles of Beninese children revealed a

430   wide variation in GYPB transcript levels and one factor that might contribute to this is

431   *GYPB* genetic polymorphisms in Africans. A high prevalence of the GPB null genotype

432   exists in malaria-endemic regions and amongst individuals of African descent – ranging

433   from 2-8% in West Africa to as high as 59% amongst the Efe pygmies in the Democratic

434   Republic of Congo (69, 70) – suggesting that malaria pressure selected for this

435   polymorphism. The Dantu variant of GPB, representing a hybrid GPA-GPB molecule

436   with a GPB N-terminal region and a GPA C-terminal region, has been shown to confer

437   protection against invasion and growth of *P. falciparum in vitro* (71). A recent study has

438   found evidence for a strong protective effect of the Dantu NE genotype against cerebral

439 malaria and severe malaria anemia in East Africa (70). The Dantu NE genotype, which

440 results from an intricate structural modification of the *GYPE-GYPB-GYPA* locus

441 including deletion of the 3' end of *GYPB*, was found to have arisen recently in Kenya. In

442 addition to the Dantu variant, the authors identified multiple examples of deletions and

443 duplications at the *GYPE-GYPB-GYPA* locus. In our study, we did not observe variation

444 in GPB surface expression in healthy Senegalese to the same extent as that seen for

445 transcription in Beninese individuals, suggesting that transcriptional differences in GYPB

446 do not directly reflect surface receptor expression. Alternatively, it is possible that there

447 are country-specific differences in GYPB polymorphisms, such that Beninese, but not

448 Senegalese individuals exhibit GYPB transcriptional variation with concomitant variation

449 in surface expression levels. Further investigation is required to understand the origin and

450 significance of GYPB transcriptional variation.

451   The observation from this work that GPB is an important receptor for *P.*

452 *falciparum* invasion is at odds with work showing that some laboratory-adapted strains

453 (72, 73) and field isolates from Kenya (74), Columbia and Peru (75) have either an *ebl-1*

454 gene deletion, a thymidine insertion or a premature stop codon that results in a truncated

455 EBL-1 product. Prior to these findings, some of the studies that had reported use of the

456 EBL-1/GPB invasion pathway had used *P. falciparum* strains that have a mutated or

457 deleted *ebl-1* gene, for example 7G8, 3D7 or HB3 (33, 35), suggesting that perhaps there

458 is an additional parasite ligand that binds to GPB. In this study, we observe usage of

459 GPB by laboratory strains that are reported to lack a functional EBL-1 ligand: 7G8, 3D7

460 (73) and HB3 (72), further suggesting that there is an additional parasite ligand for GPB.

461 Such a ligand may have features in common with the other *P. falciparum* invasion

ligands that bind glycophorins (EBA-175, EBL-1 and EBA-140), such as a DBL-like domain.

Importantly, our work demonstrates that many field strains use GPB for invasion. Given this dependence on GPB in a region with GPB null prevalence, it would be relevant to genotype field isolates to determine if there are any mutations in *ebl-1*, as has been noted in some field isolates in Kenya (74), Columbia and Peru (75), and in the absence of inactivating mutations, to determine if invasion-inhibitory EBL-1 antibodies exist in the Senegalese population. Identifying an alternate invasion ligand that binds to GPB would warrant assessing usage by field isolates and determining the ability of naturally acquired antibodies against this ligand to block invasion, which may lead to consideration of this ligand for inclusion in an invasion-blocking subunit vaccine.

Eight of the nine field strains in this study showed decreased invasion into either GPA, GPB, and/or GPC KD cells, emphasizing the sialic acid-dependent nature of many Senegalese strains. We also found that several field isolates had decreased invasion into Nm-treated pRBCs, consistent with previous field studies reporting decreased invasion of Nm-treated pRBCs (15, 18, 26, 76). However, we did not find a simple concordance between decreased invasion into GPA, GPB and GPC KD cRBCs and sialic acid-dependence (as determined by invasion into Nm-treated pRBCs) (Table S3), underscoring the importance of separately assessing specific receptors. In this study, we have investigated the use of three major sialylated receptors, and in so doing, highlighted the lesser role of GPC compared with GPA or GPB. The minor role of the EBA-140/GPC invasion pathway, especially in laboratory strains, is in concordance with other studies (21, 23). Knockout of the EBA-140 invasion ligand is facile in all laboratory strains (9),

485   and in contrast to knockouts of EBA-175, does not lead to a change in the use of ligand-

486   receptor interactions (23).   Jiang *et al*., show that chymotrypsin treatment of GPA-null

487   cells (En(a-)) causes an almost complete block in invasion of ten *P. falciparum* laboratory

488   strains (21). Both the EBA-175/GPA and the EBA-140/GPC invasion pathways are

489   chymotrypsin-resistant, indicating minimal use of the EBA-140/GPC invasion pathway in

490   the absence of GPA (21). In addition, the limited requirement of GPC for erythrocyte

491   invasion can be viewed in light of the interaction between the subtelomeric variant open

492   reading frame protein (STEVOR) and GPC (77) for the rosetting of parasite-infected

493   erythrocytes, suggesting an additional role for this erythrocyte receptor.

494   Recent studies have provided more evidence to demonstrate the importance of

495   deformability in the invasion process (78, 79). We did not measure deformability of KD

496   cRBCs, however, it is unlikely that changes in deformability of cRBCs as a result of

497   receptor KDs account for the invasion phenotypes of *P. falciparum* strains into KD

498   cRBCs. This is because GPA null cells and GPB null cells have similar deformability and

499   membrane mechanical stability as WT pRBCs (80), whereas GPC null cells reportedly

500   have decreased membrane stability and deformability (80). But the majority of *P.*

501   *falciparum* strains in this study had normal invasion into GPC KD cRBCs.

502   Altogether, the genetic evidence presented in this study reveals that the GPB

503   invasion pathway is important for invasion of strains tested. Our study provides the

504   impetus for a more detailed investigation into the use of GPB by alternative invasion

505   ligands, and the use of EBL-1 in invasion by field isolates, both of which could

506   contribute to the dominance of GPB as a receptor in the hierarchy of the RBL and EBL

507   invasion ligands.

508

526

527   **References**

528   1.   **Miller LH**, **Baruch DI**, **Marsh K**, **Doumbo OK**. 2002. The pathogenic basis of

529   malaria. Nature **415**:673–679.

530   2.   **Iyer J**, **Grüner A**, **Rénia L**, **Snounou G**, **Preiser P**. 2007. Invasion of host cells

23

531   by malaria parasites: a tale of two protein families. Mol Microbiol **65**:231–249.

532   3.   **Paul AS**, **Egan ES**, **Duarisingh MT**. 2015. Host-parasite interactions that guide

533   red blood cell invasion by malaria parasites. Curr Opin Hematol **22**:220–226.

534   4.   **Tham WH**, **Healer J**, **Cowman AF**. 2012. Erythrocyte and reticulocyte binding-

535   like proteins of *Plasmodium falciparum*. Trends Parasitol. **1**:23-30

536   5.   **Camus D**, **Hadley TJ**. 1985. A *Plasmodium falciparum* antigen that binds to host

537   erythrocytes and merozoites. Science. **230**:553–556.

538   6.   **Li X**, **Marinkovic M**, **Russo C**, **McKnight CJ**, **Coetzer TL**, **Chishti AH**. 2012.

539   Identification of a specific region of *Plasmodium falciparum* EBL-1 that binds to

540   host receptor glycophorin B and inhibits merozoite invasion in human red blood

541   cells. Mol Biochem Parasitol **183**:23–31.

542   7.   **Mayer DCG**, **Cofie J**, **Jiang L**, **Hartl DL**, **Tracy E**, **Kabat J**, **Mendoza LH**,

543   **Miller LH**. 2009. Glycophorin B is the erythrocyte receptor of *Plasmodium*

544   *falciparum* erythrocyte-binding ligand, EBL-1. Proc Natl Acad Sci **106**:5348–

545   5352.

546   8.   **Lobo CA**, **Rodriguez M**, **Reid M**, **Lustigman S**. 2003. Glycophorin C is the

547   receptor for the *Plasmodium falciparum* erythrocyte binding ligand PfEBP-2

548   (baebl). Blood **101**:4628–4631.

549   9.   **Maier AG**, **Duraisingh MT**, **Reeder JC**, **Patel SS**, **Kazura JW**, **Zimmerman**

550   **PA**, **Cowman AF**. 2003. *Plasmodium falciparum* erythrocyte invasion through

551   glycophorin C and selection for Gerbich negativity in human populations. Nat Med

552   **9**:87–92.

553   10.   **Spadafora C**, **Awandare GA**, **Kopydlowski KM**, **Czege J**, **Moch JK**, **Finberg**

554   **RW**, **Tsokos GC**, **Stoute JA**. 2010. Complement receptor 1 is a sialic acid-

555   independent erythrocyte receptor of *Plasmodium falciparum*. PLoS Pathog

556   **6(6):**e1000968

557 11. **Tham W-H**, **Wilson DW**, **Lopaticki S**, **Schmidt CQ**, **Tetteh-Quarcoo PB**,

558   **Barlow PN**, **Richard D**, **Corbin JE**, **Beeson JG**, **Cowman AF**. 2010.

559   Complement receptor 1 is the host erythrocyte receptor for *Plasmodium*

560   *falciparum* PfRh4 invasion ligand. Proc Natl Acad Sci **107**:17327–32.

561 12. **Crosnier C**, **Bustamante LY**, **Bartholdson SJ**, **Bei AK**, **Theron M**, **Uchikawa**

562   **M**, **Mboup S**, **Ndir O**, **Kwiatkowski DP**, **Duraisingh MT**, **Rayner JC**, **Wright**

563   **GJ**. 2011. Basigin is a receptor essential for erythrocyte invasion by *Plasmodium*

564   *falciparum*. Nature 4–8.

565 13. **Reed MB**, **Caruana SR**, **Batchelor AH**, **Thompson JK**, **Crabb BS**, **Cowman**

566   **AF**. 2000. Targeted disruption of an erythrocyte binding antigen in *Plasmodium*

567   *falciparum* is associated with a switch toward a sialic acid-independent pathway of

568   invasion. Proc Natl Acad Sci **97**:7509–7514.

569 14. **Stubbs J**, **Simpson KM**, **Triglia T**, **Plouffe D**, **Tonkin CJ**, **Duraisingh MT**,

570   **Maier AG**, **Winzeler EA**, **Cowman AF**. 2005. Molecular mechanism for

571   switching of *P. falciparum* invasion pathways into human erythrocytes. Science

572   **309**:1384–1387.

573 15. **Mensah-Brown H**, **Amoako N**, **Abugri J**, **Stewart L**, **Agongo G**, **Dickson E**,

574   **Ofori M**, **Stoute J**, **Conway D**, **Awandare G**. 2015. Analysis of Erythrocyte

575   Invasion Mechanisms of *Plasmodium falciparum* Clinical Isolates Across 3

576   Malaria-Endemic Areas in Ghana. J Infect Dis **212**:1288–1297.

25

577   16.   **Lobo CA**, **De Frazao K**, **Rodriguez M**, **Reid M**, **Zalis M**, **Lustigman S**. 2004.

578   Invasion profiles of Brazilian field isolates of *Plasmodium falciparum*: Phenotypic

579   and genotypic analyses. Infect Immun **72**:5886–5891.

580   17.   **Baum J**, **Pinder M**, **Conway DJ**. 2003. Erythrocyte invasion phenotypes of

581   *Plasmodium falciparum* in the Gambia. Infect Immun **71**:1856–1863.

582   18.   **Jennings C V.**, **Ahouidi AD**, **Zilversmit M**, **Bei AK**, **Rayner J**, **Sarr O**, **Ndir O**,

583   **Wirth DF**, **Mboup S**, **Duraisingh MT**. 2007. Molecular analysis of erythrocyte

584   invasion in *Plasmodium falciparum* isolates from Senegal. Infect Immun **75**:3531–

585   3538.

586   19.   **Bei A**, **Membi C**, **Rayner J**, **Mubi M**, **Ngasala B**, **Sultan A**, **Premji Z**,

587   **Duraisingh M**. 2007. Variant merozoite protein expression is associated with

588   erythrocyte invasion phenotypes in *Plasmodium falciparum* isolates from

589   Tanzania. Mol Biochem Parasitol **153**:66–71.

590   20.   **Baum J**, **Chen L**, **Healer J**, **Lopaticki S**, **Boyle M**, **Triglia T**, **Ehlgen F**, **Ralph**

591   **SA**, **Beeson JG**, **Cowman AF**. 2009. Reticulocyte-binding protein homologue 5 -

592   An essential adhesin involved in invasion of human erythrocytes by *Plasmodium*

593   *falciparum*. Int J Parasitol **39**:371–380.

594   21.   **Jiang L**, **Gaur D**, **Mu J**, **Zhou H**, **Long C a**, **Miller LH**. 2011. Evidence for

595   erythrocyte-binding antigen 175 as a component of a ligand-blocking blood-stage

596   malaria vaccine. Proc Natl Acad Sci **108**:7553–7558.

597   22.   **Healer J**, **Thompson JK**, **Riglar DT**, **Wilson DW**, **Chiu YHC**, **Miura K**, **Chen**

598   **L**, **Hodder AN**, **Long CA**, **Hansen DS**, **Baum J**, **Cowman AF**. 2013.

599   Vaccination with Conserved Regions of Erythrocyte-Binding Antigens Induces

600   Neutralizing Antibodies against Multiple Strains of *Plasmodium falciparum*. PLoS

601   One **8(9):**e72504

602 23. **Duraisingh MT**, **Maier AG**, **Triglia T**, **Cowman AF**. 2003. Erythrocyte-binding

603   antigen 175 mediates invasion in *Plasmodium falciparum* utilizing sialic acid-

604   dependent and -independent pathways. Proc Natl Acad Sci **100**:4796–801.

605 24. **Richards JS**, **Stanisic DI**, **Fowkes FJI**, **Tavul L**, **Dabod E**, **Thompson JK**,

606   **Kumar S**, **Chitnis CE**, **Narum DL**, **Michon P**, **Siba PM**, **Cowman AF**, **Mueller**

607   **I**, **Beeson JG**. 2010. Association between naturally acquired antibodies to

608   erythrocyte-binding antigens of *Plasmodium falciparum* and protection from

609   malaria and high-density parasitemia. Clin Infect Dis **51**:e50-60.

610 25. **Irani V**, **Ramsland PA**, **Guy AJ**, **Siba PM**, **Mueller I**, **Richards JS**, **Beeson JG**.

611   2015. Acquisition of Functional Antibodies That Block the Binding of

612   Erythrocyte-Binding Antigen 175 and Protection Against *Plasmodium falciparum*

613   Malaria in Children. Clin Infect Dis **61**:1244–1252.

614 26. **Badiane AS**, **Bei AK**, **Ahouidi AD**, **Patel SD**, **Salinas N**, **Ndiaye D**, **Sarr O**,

615   **Ndir O**, **Tolia NH**, **Mboup S**, **Duraisingh MT**. 2013. Inhibitory humoral

616   responses to the *Plasmodium falciparum* vaccine candidate EBA-175 are

617   independent of the erythrocyte invasion pathway. Clin Vaccine Immunol **20**:1238–

618   1245.

619 27. **Patel SD**, **Ahouidi AD**, **Bei AK**, **Dieye TN**, **Mboup S**, **Harrison SC**, **Duraisingh**

620   **MT**. 2013. *Plasmodium falciparum* merozoite surface antigen, PfRH5, elicits

621   detectable levels of invasion-inhibiting antibodies in humans. J Infect Dis

622   **208**:1679–1687.

623 28. **Jiang L**, **Duriseti S**, **Sun P**, **Miller LH**. 2009. Molecular basis of binding of the

624   *Plasmodium falciparum* receptor BAEBL to erythrocyte receptor glycophorin C.

625   Mol Biochem Parasitol **168**:49–54.

626 29. **Lin DH**, **Malpede BM**, **Batchelor JD**, **Tolia NH**. 2012. Crystal and solution

627   structures of *Plasmodium falciparum* erythrocyte-binding antigen 140 reveal

628   determinants of receptor specificity during erythrocyte invasion. J Biol Chem

629   **287**:36830–36836.

630 30. **Gilberger T**, **Thompson J**, **Triglia T**, **Good R**, **Duraisingh M**, **Cowman A**.

631   2003. A novel erythrocyte binding antigen-175 paralogue from *Plasmodium*

632   *falciparum* defines a new trypsin-resistant receptor on human erythrocytes. J Biol

633   Chem **278**:14480–14486.

634 31. **Maier AG**, **Baum J**, **Smith B**, **Conway DJ**, **Cowman AF**. 2009. Polymorphisms

635   in erythrocyte binding antigens 140 and 181 affect function and binding but not

636   receptor specificity in *Plasmodium falciparum*. Infect Immun **77**:1689–1699.

637 32. **Mayer D**, **Mu J**, **Kaneko O**, **Duan J**, **Su X**, **Miller L**. 2004. Polymorphism in the

638   *Plasmodium falciparum* erythrocyte-binding ligand JESEBL/EBA-181 alters its

639   receptor specificity. Proc Natl Acad Sci **101**:2518–2523.

640 33. **Rayner JC**, **Vargas-Serrato E**, **Huber CS**, **Galinski MR**, **Barnwell JW**. 2001.

641   A *Plasmodium falciparum* homologue of *Plasmodium vivax* reticulocyte binding

642   protein (PvRBP1) defines a trypsin-resistant erythrocyte invasion pathway. J Exp

643   Med **194**:1571–1581.

644 34. **Dolan SA**, **Proctor JL**, **Alling DW**, **Okubo Y**, **Wellems TE**, **Miller LH**. 1994.

645   Glycophorin B as an EBA-175 independent *Plasmodium falciparum* receptor of

646   human erythrocytes. Mol Biochem Parasitol **64**:55–63.

647   35. **Gaur D**, **Storry JR**, **Reid ME**, **Barnwell JW**, **Miller LH**. 2003. *Plasmodium*

648   *falciparum* Is Able to Invade Erythrocytes through a Trypsin-Resistant Pathway

649   Independent of Glycophorin B. Infect Immun **71**:6742–6746.

650   36. **Idaghdour Y**, **Quinlan J**, **Goulet JP**, **Berghout J**, **Gbeha E**, **Bruat V**, **de**

651   **Malliard T**, **Grenier JC**, **Gomez S**, **Gros P**, **Rahimy MC**, **Sanni A**, **Awadalla P**.

652   2012. Evidence for additive and interaction effects of host genotype and infection

653   in malaria. Proc Natl Acad Sci **109**:16786–16793.

654   37. **Bei AK**, **Brugnara C**, **Duraisingh MT**. 2010. *In vitro* genetic analysis of an

655   erythrocyte determinant of malaria infection. J Infect Dis **202**:1722–1727.

656   38. **Watkins NA**, **Gusnanto A**, **De Bono B**, **De S**, **Miranda-Saavedra D**, **Hardie**

657   **DL**, **Angenent WGJ**, **Attwood AP**, **Ellis PD**, **Erber W**, **Foad NS**, **Garner SF**,

658   **Isacke CM**, **Jolley J**, **Koch K**, **Macaulay IC**, **Morley SL**, **Rendon A**, **Rice KM**,

659   **Taylor N**, **Thijssen-Timmer DC**, **Tijssen MR**, **Van Der Schoot CE**, **Wernisch**

660   **L**, **Winzer T**, **Dudbridge F**, **Buckley CD**, **Langford CF**, **Teichmann S**,

661   **Göttgens B**, **Ouwehand WH**. 2009. A HaemAtlas: Characterizing gene

662   expression in differentiated human blood cells. Blood **113(19):**e1-9.

663   39. **Ritchie ME**, **Phipson B**, **Wu D**, **Hu Y**, **Law CW**, **Shi W**, **Smyth GK**. 2015.

664   Limma powers differential expression analyses for RNA-sequencing and

665   microarray studies. Nucleic Acids Res **43(7)**:e47.

666   40. **Giarratana MC**, **Rouard H**, **Dumont A**, **Kiger L**, **Safeukui I**, **Le Pennec PY**,

667   **Francois S**, **Trugnan G**, **Peyrard T**, **Marie T**, **Jolly S**, **Hebert N**, **Mazurier C**,

668   **Mario N**, **Harmand L**, **Lapillonne H**, **Devaux JY**, **Douay L**. 2011. Proof of

669　　principle for transfusion of *in vitro*-generated red blood cells. Blood **118**:5071–

670　　5079.

671　41.　**Egan ES**, **Jiang RHY**, **Moechtar MA**, **Barteneva NS**, **Weekes MP**, **Nobre L V**,

672　　**Gygi SP**, **Paulo JA**, **Frantzreb C**, **Tani Y**, **Takahashi J**, **Watanabe S**, **Goldberg**

673　　**J**, **Paul AS**, **Brugnara C**, **Root DE**, **Wiegand RC**, **Doench JG**, **Duraisingh MT**.

674　　2015. A forward genetic screen identifies erythrocyte CD55 as essential for

675　　*Plasmodium falciparum* invasion. Science **348**:711–714.

676　42.　**Douay L**, **Giarratana MC**. 2009. *Ex vivo* generation of human red blood cells: a

677　　new advance in stem cell engineering. Methods Mol Biol **482**:127–140.

678　43.　**Giarratana MC**, **Kobari L**, **Lapillonne H**, **Chalmers D**, **Kiger L**, **Cynober T**,

679　　**Marden MC**, **Wajcman H**, **Douay L**. 2005. *Ex vivo* generation of fully mature

680　　human red blood cells from hematopoietic stem cells. Nat Biotechnol **23**:69–74.

681　44.　**Weekes MP**, **Tan SYL**, **Poole E**, **Talbot S**, **Antrobus R**, **Smith DL**, **Montag C**,

682　　**Gygi SP**, **Sinclair JH**, **Lehner PJ**. 2013. Latency-Associated Degradation of the

683　　MRP1 Drug Transporter During Latent Human Cytomegalovirus Infection.

684　　Science **340**:199–202.

685　45.　**Weekes MP**, **Antrobus R**, **Talbot S**, **Hör S**, **Simecek N**, **Smith DL**, **Bloor S**,

686　　**Randow F**, **Lehner PJ**. 2012. Proteomic plasma membrane profiling reveals an

687　　essential role for gp96 in the cell surface expression of LDLR family members,

688　　including the LDL receptor and LRP6. J Proteome Res **11(3)**:1475–1484.

689　46.　**Da Costa L**, **Mohandas N**, **Sorette M**, **Grange MJ**, **Tchernia G**, **Cynober T**.

690　　2001. Temporal differences in membrane loss lead to distinct reticulocyte features

691　　in hereditary spherocytosis and in immune hemolytic anemia. Blood **98**:2894–

692 2899.

693 47. **Weekes MP**, **Tomasec P**, **Huttlin EL**, **Fielding CA**, **Nusinow D**, **Stanton RJ**,

694 **Wang ECY**, **Aicheler R**, **Murrell I**, **Wilkinson GWG**, **Lehner PJ**, **Gygi SP**.

695 2014. Quantitative temporal viromics: An approach to investigate host-pathogen

696 interaction. Cell **157**:1460–1472.

697 48. **The Uniprot C**. 2017. UniProt: the universal protein knowledgebase. Nucleic

698 Acids Res **45**:D158–D169.

699 49. **Sonnhammer EL**, **von Heijne G**, **Krogh A**. 1998. A hidden Markov model for

700 predicting transmembrane helices in protein sequences. Proc Int Conf Intell Syst

701 Mol Biol **6**:175–182.

702 50. **Krogh A**, **Larsson B**, **Heijne G**, **Sonnhammer EL**. 2001. Predicting

703 transmembrane protein topology with a hidden Markov model: application to

704 complete genomes. J Mol Biol **305**:567–580.

705 51. **Cox J**, **Mann M**. 2008. MaxQuant enables high peptide identification rates,

706 individualized p.p.b.-range mass accuracies and proteome-wide protein

707 quantification. Nat Biotechnol **26**:1367–72.

708 52. **de Hoon MJL**, **Imoto S**, **Nolan J**, **Miyano S**. 2004. Open source clustering

709 software. Bioinformatics **20**:1453–1454.

710 53. **Saldanha AJ**. 2004. Java Treeview - Extensible visualization of microarray data.

711 Bioinformatics **20**:3246–3248.

712 54. **Bei AK**, **Duraisingh MT**. 2012. Functional analysis of erythrocyte determinants

713 of *Plasmodium* infection. Int J Parasitol. **42(6):**575-582

714 55. **Johnstone RM**, **Adam M**, **Hammond JR**, **Orr L**, **Turbide C**. 1987. Vesicle

715   formation during reticulocyte maturation. Association of plasma membrane

716   activities with released vesicles (exosomes). J Biol Chem **262**:9412–9420.

717 56. **Serke S**, **Huhn D**. 1992. Identification of CD71 (transferrin receptor) expressing

718   erythrocytes by multiparameter-flow-cytometry (MP-FCM): correlation to the

719   quantitation of reticulocytes as determined by conventional microscopy and by

720   MP-FCM using a RNA-staining dye. Br J Haematol **81**:432–439.

721 57. **Okumura N**, **Tsuji K**, **Nakahata T**. 1992. Changes in cell surface antigen

722   expressions during proliferation and differentiation of human erythroid

723   progenitors. Blood **80**:642–50.

724 58. **Li J**, **Hale J**, **Bhagia P**, **Xue F**, **Chen L**, **Jaffray J**, **Yan H**, **Lane J**, **Gallagher**

725   **PG**, **Mohandas N**, **Liu J**, **An X**. 2014. Isolation and transcriptome analyses of

726   human erythroid progenitors: BFU-E and CFU-E. Blood **124**:3636–3645.

727 59. **Griffiths RE**, **Kupzig S**, **Cogan N**, **Mankelow TJ**, **Betin VMS**, **Trakarnsanga**

728   **K**, **Massey EJ**, **Lane JD**, **Parsons SF**, **Anstee DJ**. 2012. Maturing reticulocytes

729   internalize plasma membrane in glycophorin A-containing vesicles that fuse with

730   autophagosomes before exocytosis. Blood **119**:6296–6306.

731 60. **Anstee DJ**, **Gardner B**, **Spring F**, **Holmes C**, **Simpson K**, **Parsons S**, **Mallinson**

732   **G**, **Yousaf S**, **Judson P**. 1991. New monoclonal antibodies in CD44 and CD58:

733   their use to quantify CD44 and CD58 on normal human erythrocytes and to

734   compare the distribution of CD44 and CD58 in human tissues. Immunology

735   **74**:197–205.

736 61. **Marion Reid Christine Lomas-Francis Martin Olsson**. 2013. The Blood Group

737   Antigen FactsBook. Lab Medicine **44(4):**e92-e96

738   62.   **Anstee DJ**. 1990. The nature and abundance of human red cell surface

739   glycoproteins. J Immunogenet **17**:219–225.

740   63.   **Baum J**, **Maier AG**, **Good RT**, **Simpson KM**, **Cowman AF**. 2005. Invasion by

741   *P. falciparum* merozoites suggests a hierarchy of molecular interactions. PLoS

742   Pathog **1(4)**:e37.

743   64.   **Satchwell TJ**. 2016. Erythrocyte invasion receptors for *Plasmodium falciparum*:

744   New and old. Transfus Med **26**:77–88.

745   65.   **Smythe J**, **Gardner B**, **Anstee DJ**. 1994. Quantitation of the number of molecules

746   of glycophorins C and D on normal red blood cells using radioiodinated Fab

747   fragments of monoclonal antibodies. Blood **83**:1668–1672.

748   66.   **Gardner B**, **Parsons SF**, **Merry AH**, **Anstee DJ**. 1989. Epitopes on

749   sialoglycoprotein alpha: evidence for heterogeneity in the molecule. Immunology

750   **68**:283–289.

751   67.   **Nigg E**, **Bron C**, **Girardet M**, **Cherry R**. 1980. Band 3-glycophorin A association

752   in erythrocyte membranes demonstrated by combining protein diffusion

753   measurements with antibody-induced cross-linking. Biochemistry **19**:1887–1893.

754   68.   **Young MT**, **Beckmann R**, **Toye a M**, **Tanner MJ**. 2000. Red-cell glycophorin

755   A-band 3 interactions associated with the movement of band 3 to the cell surface.

756   Biochem J **350 Pt 1**:53–60.

757   69.   **Giblett E**, **Motusky A**, **Fraser G**. 1966. Population genetic studies in the Congo.

758   IV. Haptoglobin and transferrin serum groups in the Congo and in other African

759   populations. Am J Hum Genet **18**:553–558.

760   70.   **Leffler E**, **Ziyue G**, **Pfeifer S**, **Segurel L**, **Auton A**, **Oliver V**, **Bowden R**,

Bontrop R, Wall J, Sella G, Donnelly P, McVean G, Przeworski M. 2017.
Multiple Instances of Ancient Balancing Selection Shared Between Humans and
Chimpanzees. Science **339**:1578–1582.

71. Field SP, Hempelmann E, Mendelow B V, Fleming AF. 1994. Glycophorin
variants and *Plasmodium falciparum*: protective effect of the Dantu phenotype *in
vitro*. Hum Genet **93**:148–150.

72. Peterson DS, Wellems TE. 2000. EBL-1, a putative erythrocyte binding protein
of *Plasmodium falciparum*, maps within a favored linkage group in two genetic
crosses. Mol Biochem Parasitol **105**:105–113.

73. Drummond P, Peterson D. 2005. An analysis of genetic diversity within the
ligand domains of the *Plasmodium falciparum* ebl-1 gene. Mol Biochem Parasitol
140:241–245.

74. Githui EK, Peterson DS, Aman RA, Abdi AI. 2010. Prevalence of 5' insertion
mutants and analysis of single nucleotide polymorphism in the erythrocyte
binding-like 1 (ebl-1) gene in Kenyan *Plasmodium falciparum* field isolates. Infect
Genet Evol **10**:833–838.

75. Lopez-Perez M, Villasis E, Machado RLD, Póvoa MM, Vinetz JM, Blair S,
Gamboa D, Lustigman S. 2012. *Plasmodium falciparum* Field Isolates from
South America Use an Atypical Red Blood Cell Invasion Pathway Associated with
Invasion Ligand Polymorphisms. PLoS One **7(10):**47913.

76. Bowyer PW, Stewart LB, Aspeling-Jones H, Mensah-Brown HE, Ahouidi AD,
Amambua-Ngwa A, Awandare GA, Conway DJ. 2015. Variation in
Plasmodium falciparum erythrocyte invasion phenotypes and merozoite ligand

784   gene expression across different populations in areas of malaria endemicity. Infect

785   Immun **83**:2575–2582.

786   77.   **Niang M**, **Bei AK**, **Madnani KG**, **Pelly S**, **Dankwa S**, **Kanjee U**, **Gunalan K**,

787   **Amaladoss A**, **Yeo KP**, **Bob NS**, **Malleret B**, **Duraisingh MT**, **Preiser PR**. 2014.

788   STEVOR is a *Plasmodium falciparum* erythrocyte binding protein that mediates

789   merozoite invasion and rosetting. Cell Host Microbe **16**:81–93.

790   78.   **Koch M**, **Wright KE**, **Otto O**, **Herbig M**, **Salinas ND**, **Tolia NH**, **Satchwell TJ**,

791   **Guck J**, **Brooks NJ**, **Baum J**. 2017. *Plasmodium falciparum* erythrocyte-binding

792   antigen 175 triggers a biophysical change in the red blood cell that facilitates

793   invasion. Proc Natl Acad Sci **114(16):**4225-4230

794   79.   **Sisquella X**, **Nebl T**, **Thompson JK**, **Whitehead L**, **Malpede BM**, **Salinas ND**,

795   **Rogers K**, **Tolia NH**, **Fleig A**, **O'Neill J**, **Tham WH**, **Horgen FD**, **Cowman AF**.

796   2017. *Plasmodium falciparum* ligand binding to erythrocytes induce alterations in

797   deformability essential for invasion. Elife **6**:e21083

798   80.   **Reid ME**, **Chasis JA**, **Mohandas N**. 1987. Identification of a functional role for

799   human erythrocyte sialoglycoproteins beta and gamma. Blood **69**:1068–1072.

800

801   **Figure Legends**

802
803   **Figure 1. Glycophorin B transcriptional variation and erythrocyte receptor**

804   **expression amongst individuals in malaria-endemic regions. A**. Graph highlighting

805   transcripts, including GYPB, whose abundance varied widely amongst erythroid-specific

806   transcripts from 61 healthy individuals in Benin. Bioinformatic analysis was based on the

807   whole blood transcriptomics study of malaria-infected and healthy children in Benin (36).

35

808   **B**. Expression of GPB and other erythrocyte receptors from blood of healthy Senegalese

809   donors in 2011 (left graph) and 2012 (right graph). The graphs show the 95/5 quantile

810   ratio normalized to the quantile ratio for a control secondary antibody. The quantile ratio

811   was based on mean fluorescence intensity values determined by flow cytometry. In 2011,

812   measurements were made on RBCs from 29 donors (GPB) or 32 donors (CD55, CR1) or

813   41 donors (RhD), and in 2012, on 11 donors (GPB) or 29 donors (all other receptors). In

814   2011, one GPB null individual and three RhD null individuals were observed but were

815   excluded from measurement of the 95/5 quantile ratio. In 2012, three different probes

816   were used to measure expression of GPA and GPC (see Materials and Methods).

817

818   **Figure 2. Knockdown of glycophorin A, B and C in cultured erythrocytes**. **A**.

819   Expression of glycophorin A (GPA), glycophorin B (GPB) and glycophorin C (GPC) on

820   the cell surface of GPA knockdown (KD) (green), GPB KD (blue) and GPC KD (pink)

821   cultured erythrocytes (cRBCs) as determined by flow cytometry. Representative flow

822   cytometry plots are shown. Grey traces: receptor expression on pLKO cRBCs; dashed

823   traces: pLKO cells stained with a control antibody. **B.** Mean expression ± standard error

824   from three to seven independent experiments, normalized to expression on pLKO cells.

825   For measurement of GPB expression, cRBCs were treated with trypsin to remove GPA

826   and cells stained with a GPA/B antibody. Statistical significance was determined using a

827   one-way analysis of variance (ANOVA) with a Dunnett's multiple comparison test.

828   Significant differences are indicated by ***$P \leq 0.001$. **C.** May-Grünwald, Giemsa-stained

829   cytospins showing normal morphology of KD and pLKO control cRBCs. cRBCs were

830   passed through a 5 µm filter to remove nucleated cells prior to flow cytometry and

831   cytospin preparation.

832

833   **Figure 3. Quantitative cell surface proteomics of peripheral erythrocytes and**

834   **cultured erythrocytes. A.** Quantitative cell surface proteomic comparison between

835   pLKO cRBCs and peripheral RBCs (pRBCs). K-means clustering analysis of the 78

836   surface membrane proteins identified three clusters: cluster 1 – proteins that decrease

837   between pLKO cRBCs and pRBCs; cluster 2 – proteins that remain at the same level

838   between pLKO cRBCs and pRBC; and cluster 3 – proteins that increase between pLKO

839   cRBCs and pRBCs. Scale bar represents normalized relative abundance of each protein.

840   Note that the peptides detected by this technique did not allow a distinction to be made

841   between GPA and GPB. **B – D.** Comparison of the relative abundance of membrane

842   proteins between the pLKO control cRBCs and either the GPA KD cRBCs **(B)**, GPB KD

843   cRBCs **(C)** or GPC KD cRBCs **(D)**. Fold change was calculated as: signal:noise (GP

844   KD)/average signal:noise (pLKO control). Y-axes show the average signal:noise (S:N)

845   across all samples. *P*-values were estimated using Benjamini-Hochberg corrected

846   Significance A, calculated in Perseus v 1.5.1.6.

847

848   **Figure 4. Schematic of invasion assay design**. **A**. A ring stage parasite culture is treated

849   with neuraminidase (N), trypsin (T) and chymotrypsin (C), returned to culture conditions

850   and allowed to mature to late trophozoite (troph) or schizont stage. The NTC-treated

851   culture (donor cells) is mixed in an 80:20 ratio with either knockdown (KD) or control

852   pLKO cRBCs (acceptor cells). Initial parasitemia and/or final parasitemia after one round

853   of invasion are determined either by microscopy from counts of 500-2000 erythrocytes or

854   by flow cytometry of SYBR green I-stained cells. Invasion assays are set up at 0.5%

855   hematocrit. All acceptor cells are counted by hemocytometer prior to assay setup. **B**.

856   Invasion of NTC-treated *P. falciparum* 3D7 into pLKO control cRBCs with varying ratio

857   of enzyme-treated donor cells to pLKO acceptor cells. 100:0 ratio indicates NTC-treated

858   3D7 donor cells and no pLKO cRBCs. Initial parasitemia was ~2%. Final parasitemia

859   was determined by flow cytometry of SYBR green I-stained cells. The assay was

860   performed once in duplicate. Bars represent the mean ± the range. The 80:20 ratio was

861   selected for subsequent invasion assays. E: Expected parasitemia based on invasion into

862   50:50 mixture. O: Observed parasitemia.

863
864
865
866
867
868
869
870
871
872
873
874
875
876
877
878
879
880
881
882
883
884
885
886
887

Table 1. Comparison of copies per unit surface area of known *P. falciparum* host receptors on peripheral erythrocytes and cultured erythrocytes.

	Copies/μm^2				
Protein	**pRBC**	**pLKO**	**GPA KD**	**GPB KD**	**GPC KD**
GPA[62-64, 66]	7.49×10^3	4.42×10^3	1.25×10^3	1.62×10^3	2.38×10^3
GPB[62-64, 66]	1.87×10^3	1.11×10^3	3.11×10^2	4.05×10^2	5.95×10^2
GPC[62-64, 65]	7.49×10^2	2.57×10^2	1.52×10^2	1.62×10^2	9.51×10^1
BSG[61, 64]	2.25×10^1	6.26×10^1	8.72×10^1	2.21×10^1	6.52×10^1
CR1[64]	$1.50 - 8.98 \times 10^0$	$0.31 - 1.84 \times 10^0$	$0.41 - 2.43 \times 10^0$	$0.38 - 2.31 \times 10^0$	$0.52 - 3.13 \times 10^0$
Band 3[61]	7.49×10^3	3.53×10^3	4.68×10^3	1.97×10^3	3.26×10^3
Kx[61]	7.49×10^0	8.81×10^0	1.05×10^1	7.04×10^0	8.36×10^0
CD55[61]	1.50×10^2	1.59×10^2	1.49×10^2	9.47×10^1	1.42×10^2
CD44[60, 61]	2.62×10^1	4.47×10^1	6.66×10^1	3.05×10^1	3.64×10^1

The reported number of copies of known *P. falciparum* host receptors on peripheral erythocytes (pRBCs) were used to estimate the number of copies of host receptors on pLKO cRBCs based on the normalized signal:noise ratios from quantitative surface proteomics and the following reported surface areas for mature RBCs: 133.6 ± 3.0 μm^2 and for reticulocytes: 142.4 ± 2.0 μm^2 (46), which we assume to be representative of pLKO cRBCs. Since GPA and GPB peptides are indistinguishable by surface proteomics, estimation was based on the reported relative abundance of GPA and GPB on pRBCs. The densities of host receptors per unit surface area for GPA, GPB, and GPC are within three-fold lower on pLKO cRBCs compared to pRBCs.

906 **Table 2. Invasion efficiency of *P. falciparum* laboratory-adapted strains and a**

907 **Senegalese culture-adapted isolate into knockdown cultured erythrocytes.**

Strain	% Invasion Efficiency[a]		
	GPA KD	GPB KD	GPC KD
Dd2	72.9 ± 18.3*	56.4 ± 24.2**	91.8 ± 8.2
3D7	90.2 ± 11.4	66.6 ± 23.3***	89.6 ± 9.8
3D7ΔEBA175	100.4 ± 31.8	53.4 ± 30.0	94.1 ± 16.5
3D7ΔRh2b	101.2 ± 14.8	60.5 ± 26.6*	100.2 ± 4.8
7G8	85.0 ± 31.5	56.1 ± 26.8	98.3 ± 21.9
HB3	101.3 ± 43.7	53.6 ± 18.1	93.0 ± 15.5
Sen51	109.7 ± 28.3	58.8 ± 16.8*	113.0 ± 3.6

910 [a]Invasion efficiency into KD cells relative to pLKO control cells; based on final

911 parasitemia. Parasitemia was determined by microscopy from counts of 500-2000

912 erythrocytes, depending on the experiment. Invasion assays were performed in triplicate,

913 four to six times for 3D7, Dd2, 7G8, and HB3 and three times for 3D7ΔEBA-175,

914 3D7ΔRh2b, and Sen51. Shown are the mean and standard deviation. Statistical

915 significance was determined using a one-way ANOVA with a Dunnett's multiple

916 comparison test. Significant differences are indicated by $*P < 0.05$, $**P \leq 0.01$ and $***P$

917 ≤ 0.001.

918
919
920

921
922
923
924
925
926
927
928
929
930
931
932

933   Table 3. Invasion efficiency of *P. falciparum ex vivo* field isolates into knockdown

934   cultured erythrocytes.

	% Invasion Efficiency[a]		
Strain	**GPA KD**	**GPB KD**	**GPC KD**
Th266	88.7 ± 12.1	66.2 ± 14.2	52.5 ± 16.4
Th268	100.9 ± 28.1	79.1 ± 17.8	54.8 ± 9.4
Th275	110.4 ± 60.7	118.0 ± 66.4	70.9 ± 10.0
Th303	39.0 ± 4.1	55.6 ± 4.6	69.1 ± 2.5
Th304	40.7 ± 1.6	56.0 ± 4.7	92.3 ± 24.9
Th305	30.6 ± 0	36.7 ± 5.8	86.7 ± 10.1
Th306	44.9 ± 0.1	47.6 ± 16.5	93.5 ± 42.2
Th312	28.5 ± 3.5	51.7 ± 10.1	91.8 ± 2.0

935

936   [a]Invasion efficiency into KD cells relative to pLKO control cells; based on final

937   parasitemia. Parasitemia was determined by microscopy from counts of 800-1000

938   erythrocytes. Invasion assays were performed once, in triplicate (Th266, Th268, Th275)

939   or duplicate (Th303, Th304, Th305, Th306, Th312). Errors indicate the standard

940   deviation (Th266, Th268, Th275) or the range (Th303, Th304, Th305, Th306, Th312).
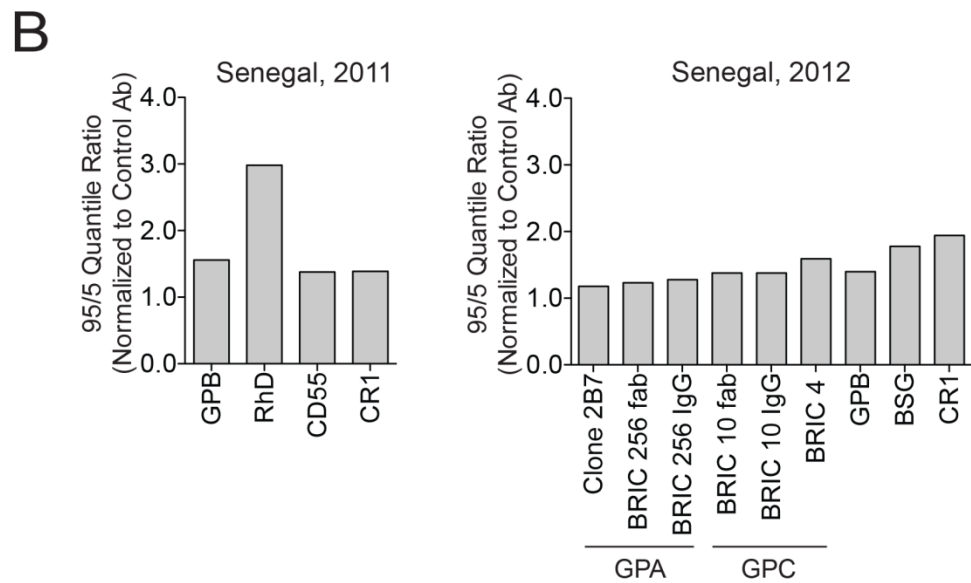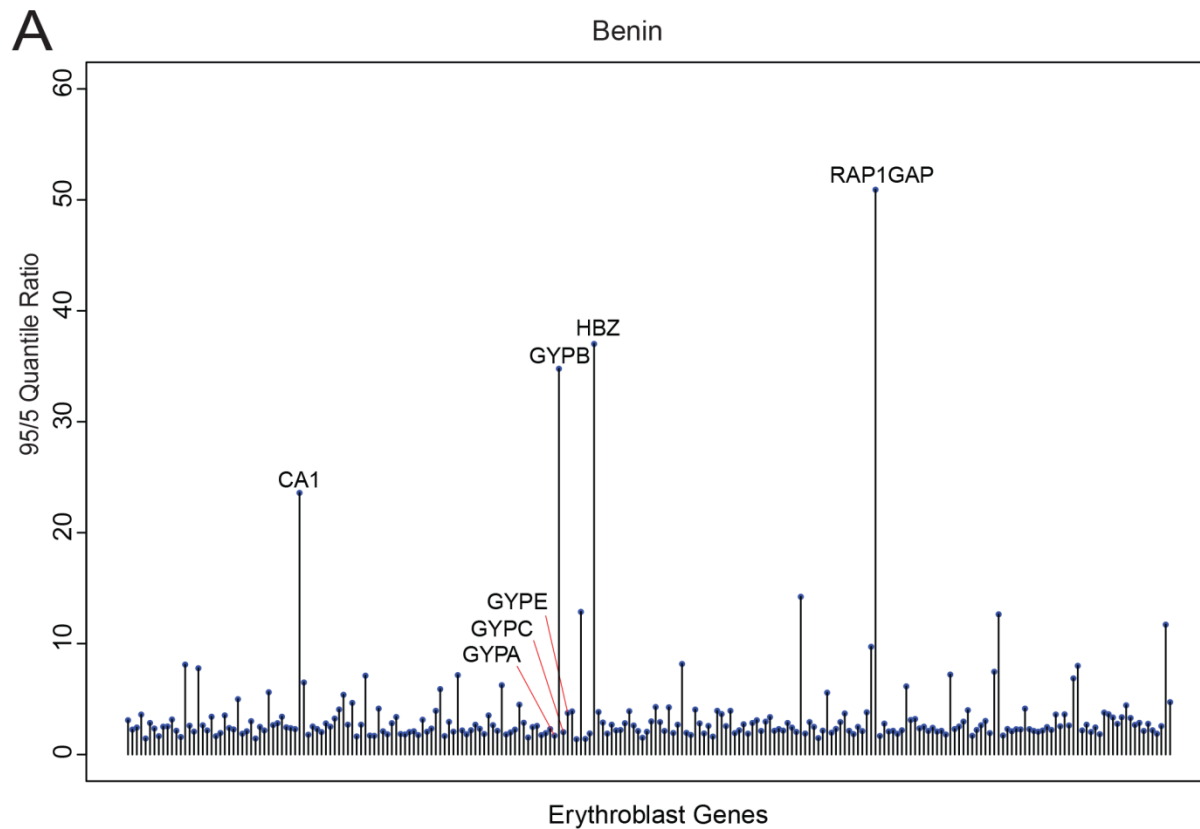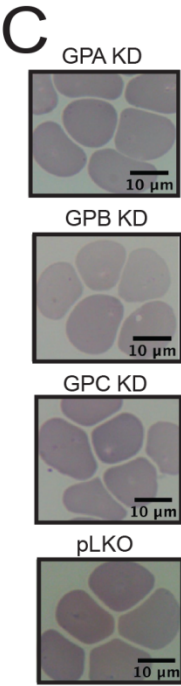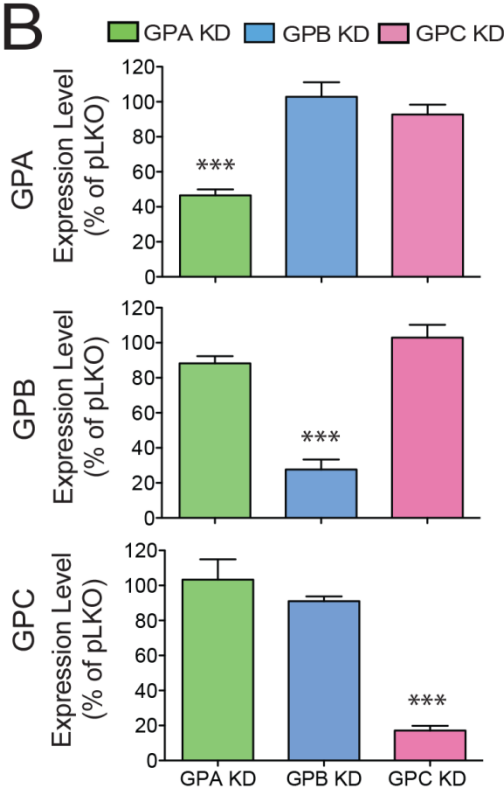
Figure 1

A Benin

B Senegal, 2011   Senegal, 2012

Figure 2

Figure 3

Figure 4

A

Ring culture → NTC treatment → Enzyme-treated Ring culture → 36-42hrs → Enzyme-treated trophs/schizonts → 80:20 ← cRBCs

cRBCs

Donor Cells + Acceptor Cells → 30-40hrs → Measurement of Re-invasion: Microscopy or Flow cytometry

B

3D7 invasion

E: 2.9 2.2 1.5 0.0
O: 3.0 2.1 0.7 0.2

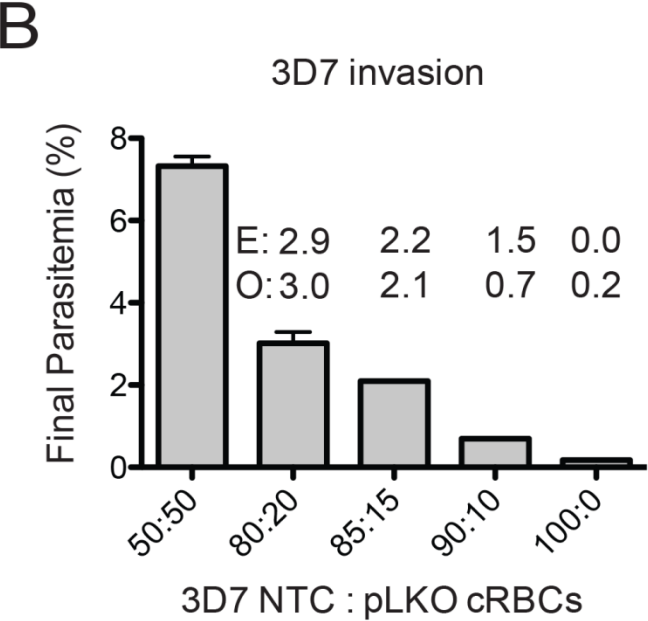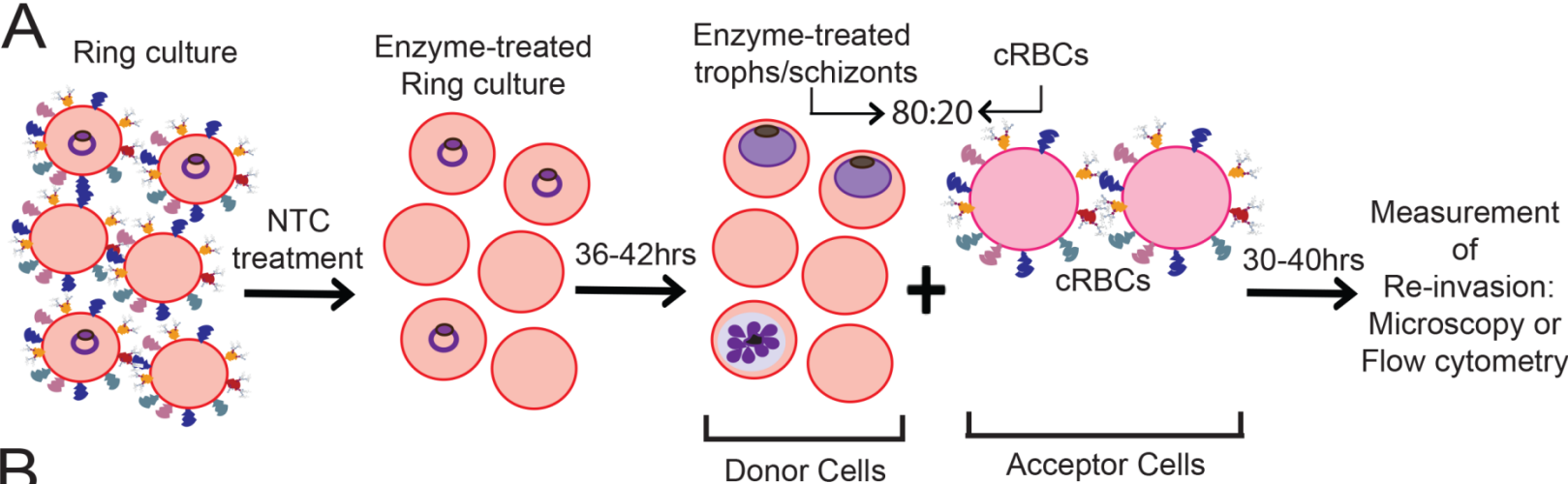Final Parasitemia (%) vs 3D7 NTC : pLKO cRBCs
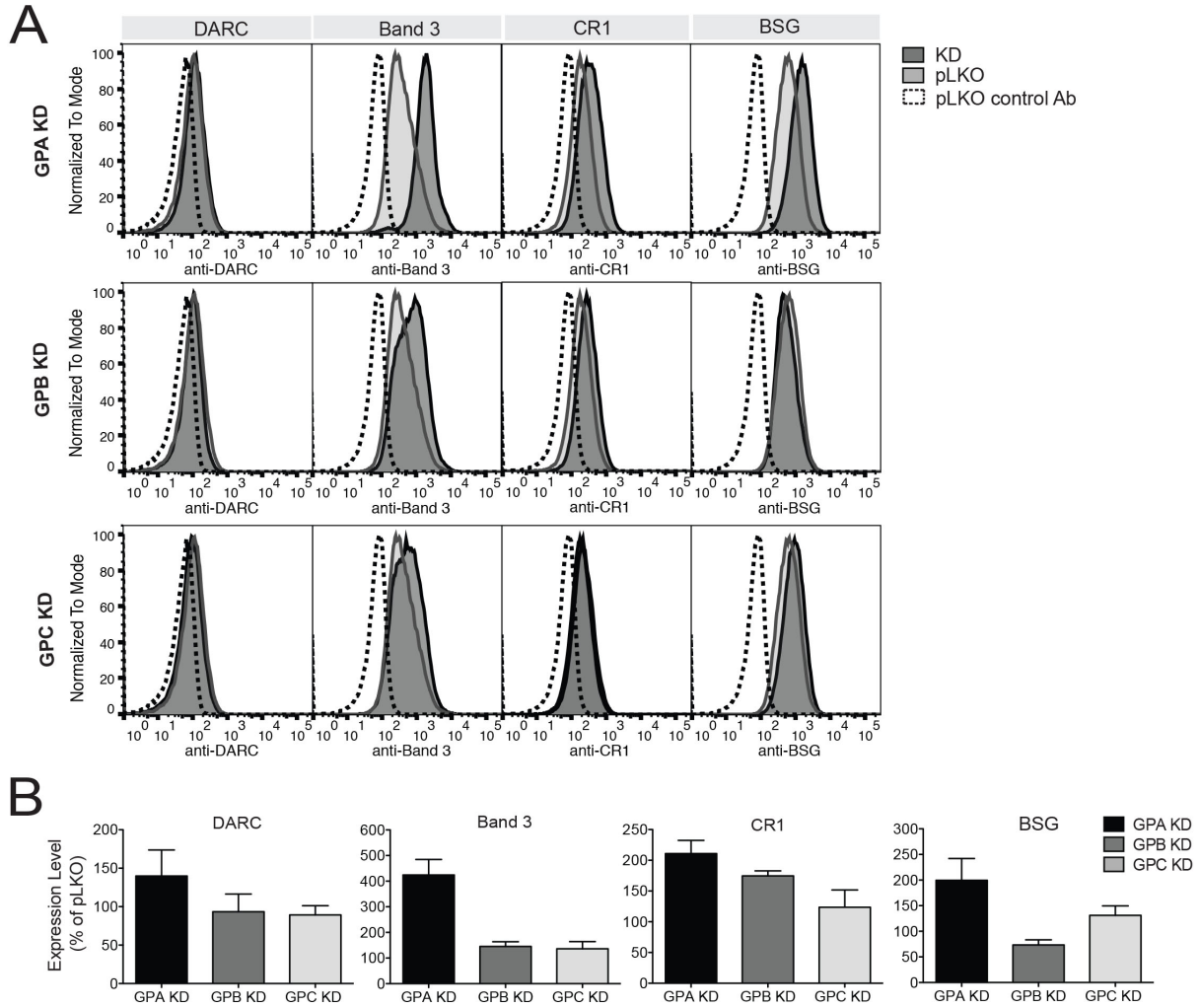
50:50, 80:20, 85:15, 90:10, 100:0
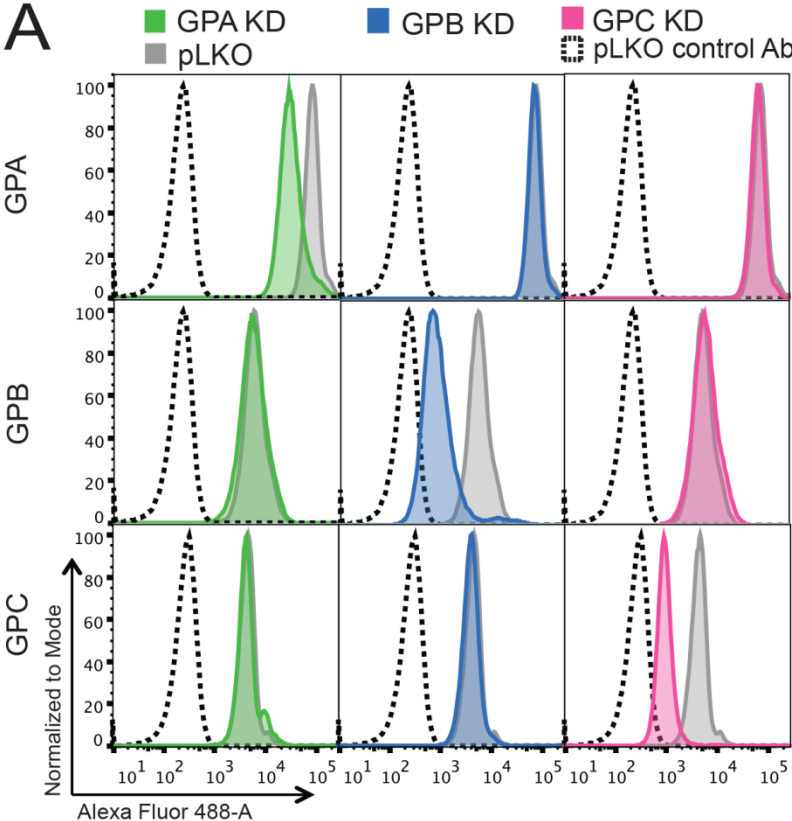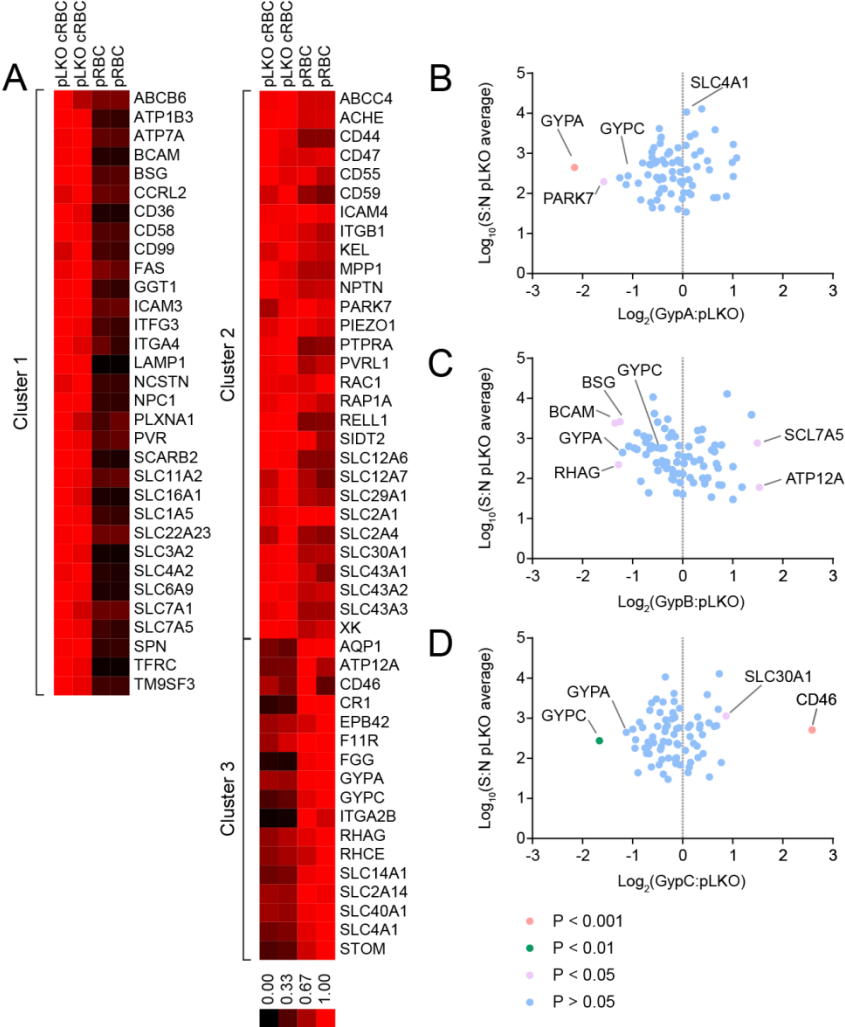
FIGURE S1. Characterization of glycophorin A-, B- and C-depleted cultured erythrocytes. A. Expression of *P. falciparum* invasion receptors (CR1 and BSG), band 3 and *P. vivax* receptor DARC on the surface of GPA KD, GPB KD and GPC KD cRBCs as determined by flow cytometry. Representative plots are shown. **B.** Mean expression ± standard deviation of *P. falciparum* invasion receptors (CR1 and BSG), DARC and band 3 receptors on the surface of GPA KD, GPB KD and GPC KD cRBCs as determined by flow cytometry from two to four experiments. cRBCs were passed through a 5 µm filter to remove nucleated cells prior to flow cytometry.

TABLE S2. Description of proteins with significant fold change in abundance.

cRBCs	Protein	Change	*P*-value	Description	Function/ Role
GPA KD	PARK7	Decreased	0.0141	Protein DJ-1	Positive regulator of androgen receptor-dependent transcription.
GPB KD	BCAM	Decreased	0.0312	Basal Cell Adhesion Molecule, Lutheran Blood Group	Member of the immunoglobulin superfamily. Receptor for the laminin extracellular matrix protein.
GPB KD	RHAG	Decreased	0.0418	Ammonium transporter Rh type A	Transport of ammonium and carbon dioxide across the erythrocyte membrane.
GPB KD	BSG	Decreased	0.0474	Basigin, Ok Blood Group	Essential role in *P. falciparum* invasion of erythrocytes.
GPB KD	SLC7A5	Increased	0.0381	Large neutral amino acids transporter small subunit 1	Transport of large neutral amino acids.
GPB KD	ATP12A	Increased	0.0336	Isoform 2 of Potassium-transporting ATPase alpha chain 2	ATPase, H+/K+ transporter.
GPC KD	SLC30A1	Increased	0.0464	Zinc transporter 1	Transport of sugars, bile salts and organic acids, metal ions and amine compounds.
GPC KD	CD46	Increased	1.8441×10^7	Complement Membrane Cofactor Protein	Complement regulatory protein.

TABLE S3. Table of neuraminidase sensitivity of *P. falciparum* strains.

Strain	IE into Nm pRBCs[a]	Resistant/Sensitive[b]	Refs
Dd2	N/A	S	(1)
3D7	N/A	R	(2)
3D7ΔEBA175	N/A	R	(2)
3D7ΔRh2b	N/A	R	(3)
7G8	N/A	R	(4)
HB3	N/A	R	(1)
Sen51	50.8 ± 8.8	S	This Study
Th266	17.3 ± 7.5	S	This Study
Th268	51.1 ± 6.3	S	This Study
Th303	45.3 ± 11.4	S	This Study
Th304	105.6 ± 4.6	R	This Study
Th305	48.9 ± 7.6	S	This Study
Th306	14.1 ± 3.1	S	This Study
Th312	61.4 ± 22	R	This Study

[a]Invasion efficiency into neuraminidase-treated (Nm) pRBCs relative to untreated pRBCs; based on final parasitemia. Parasitemia was determined by SYBR green flow cytometry. Mean ± standard deviation (Sen51, Th266, Th268) or range (Th303, Th304, Th305, Th306, Th312) for one biological replicate.

[b]Sensitivity to neuraminidase treatment for field isolates in this study was based on a cutoff of 60%.

References

1. Dolan SA, Proctor JL, Alling DW, Okubo Y, Wellems TE, Miller LH. 1994. Glycophorin B as an EBA-175 independent Plasmodium falciparum receptor of human erythrocytes. Mol Biochem Parasitol 64:55-63.
2. Duraisingh MT, Maier AG, Triglia T, Cowman AF. 2003. Erythrocyte-binding antigen 175 mediates invasion in Plasmodium falciparum utilizing sialic acid-dependent and - independent pathways. Proc Natl Acad Sci U S A 100:4796-801.
3. Duraisingh MT, Triglia T, Ralph SA, Rayner JC, Barnwell JW, McFadden GI, Cowman AF. 2003. Phenotypic variation of Plasmodium falciparum merozoite proteins directs receptor targeting for invasion of human erythrocytes. Embo J 22:1047-57.
4. Hadley TJ, Klotz FW, Pasvol G, Haynes JD, McGinniss MH, Okubo Y, Miller LH. 1987. Falciparum malaria parasites invade erythrocytes that lack glycophorin A and B (MkMk). Strain differences indicate receptor heterogeneity and two pathways for invasion. J Clin Invest 80:1190-3.